JOURNAL OF BACTERIOLOGY, May 1994, p. 2807–2813
0021-9193/94/$04.00+0

Vol. 176, No. 10

The RNA Chain Elongation Rate in *Escherichia coli* Depends on the Growth Rate

ULLA VOGEL AND KAJ FRANK JENSEN*

Department of Biological Chemistry, Institute of Molecular Biology, University of Copenhagen, Copenhagen, Denmark

Received 24 November 1993/Accepted 10 March 1994

We determined the rates of mRNA and protein chain elongation on the *lacZ* gene during exponential growth on different carbon sources. The RNA chain elongation rate was calculated from measurements of the time elapsing between induction of *lacZ* expression and detection of specific hybridization with a probe near the 3′ end of the mRNA. The elongation rate for the transcripts decreased 40% when the growth rate decreased by a factor of 4, and it always correlated with the rate of translation elongation. A similar growth rate dependency was seen for transcription on the *infB* gene and on a part of the *rrnB* gene fused to a synthetic, inducible promoter. However, the untranslated RNA chain specified by the *rrnB* gene was elongated nearly twice as fast as the two mRNA species encoded by *infB* and *lacZ*.

The rate of RNA chain elongation in *Escherichia coli* is generally regarded as being constant and independent of the growth rate, while it is well accepted that the polypeptide chain growth rate depends on the medium (5). It is known that decoupling of translation from transcription causes premature mRNA chain termination in several genes and operons (1) and that a tight coupling between RNA polymerase and the leading ribosome is able to suppress transcriptional pausing and termination at attenuators of amino acid and nucleotide biosynthetic genes (16, 19, 20, 29). Since premature transcription termination does not seem to prevail during steady-state growth, one might expect that rates of transcription and translation were very tightly adjusted to each other in steady-state cultures. Therefore, we wanted to measure the transcription elongation rate during exponential growth in different media.

MATERIALS AND METHODS

Bacterial strains and plasmids. Strain MAS90 is *E. coli* K-12 *thi* Δ*pro-lac recA1*/F′ *lacI*^{q1} *lacZ*::Tn*5* *proAB*$^{+}$ and was previously described (39). As used here, MAS90 was transformed with different plasmids, pMAS2 (34), pUV12, pUV14, and pUV17 (37), which all encode resistance to ampicillin.

Growth conditions. The experimental cultures were started by dilution of exponentially growing cultures in the same medium. Cultures were grown in shaking Erlenmeyer flasks at 37°C. The medium was either Luria-Bertani (LB) (24) containing 100 μg of ampicillin per ml (doubling time, 24 min) or the A+B salt medium of Clark and Maaløe (7). This salt medium was supplemented with ampicillin (100 μg/ml) and thiamine (1 μg/ml) and one of the following carbon sources: succinate (0.4%) (doubling time, 160 min), glycerol (0.4%) (doubling time, 78 min), glucose (0.1%) (doubling time, 58 min), glycerol (0.4%) plus Casamino Acids (0.2%) (doubling time, 50 min), or glucose (0.2%) plus Casamino Acids (0.2%) (doubling time, 35 min). For some experiments the cells were grown with glucose at 0.1% plus α-methylglucoside at 0.5% (doubling time, 120 min) or glucose at 0.1% plus α-methylglucoside at 1.5% (doubling time, 200 min).

Determination of induction lag for β-galactosidase. Transcription from *lacZ* was induced by addition of 1 mM isopropyl-β-D-thiogalactoside (IPTG) at time zero. Subsequently, at 10-s intervals, samples (0.5 ml) of the culture were pipetted into precooled Eppendorf tubes containing 3 μl of chloramphenicol (34 g/liter) to stop protein chain elongation. The cells were disrupted by ultrasonic treatment for 30 s in the growth medium. The β-galactosidase activities were determined as described by Miller (24), and the data were analyzed in the square-root plot of Schleif et al. (31).

Preparation of RNA and dot blot analysis. For determination of the RNA chain growth kinetics, 4-ml samples were withdrawn for RNA purification at 10-s intervals after induction of transcription as described by Vogel et al. (39). The RNA samples were analyzed by dot blot hybridization on GeneScreen membranes with different radioactive RNA probes (37). In short, 5 μg of RNA was dissolved in 50% deionized formamide containing 6% formaldehyde, denatured, and applied on a dot blot manifold. The RNA was fixed to the membrane by UV irradiation for 2 min and prehybridized without drying. Prehybridization, hybridization with ^{32}P-labelled RNA probes, and subsequent washing were performed as described elsewhere (37). The wet membranes were subjected to autoradiography, the radioactive dots were cut out, and the amount of hybridization to each dot was quantified by liquid scintillation counting. Blank samples were used to determine the background and subtracted from all values. This background was usually 30 to 40 cpm.

Two parallel dot blots were performed, one using a ^{32}P-labelled riboprobe complementary to the 3′ end of the induced transcript and another using a probe complementary to the constitutive *bla* transcript. The amount of radioactivity retained in the dot hybridizing with the induced RNA chain (i.e., *lacZ* or *cat*) was normalized by dividing by the corresponding amount of radioactivity retained by the constitutive *bla* mRNA. Normalization relative to the *bla* mRNA was necessary for the experiments with pMAS2 but was unnecessary for pUV12, pUV14, and pUV17, which carry the very strong $P_{A1/04/03}$ promoter. (The absolute ratio *lacZ*/*bla* or *cat*/*bla* should not be interpreted in terms of promoter activity, as the absolute amount of accumulated RNA levels depends on the RNA

* Corresponding author. Mailing address: Department of Biological Chemistry, Institute of Molecular Biology, Sølvgade 83H, DK-1307 Copenhagen K, Denmark. Electronic mail address: kfj@mermaid.molbio.ku.dk.

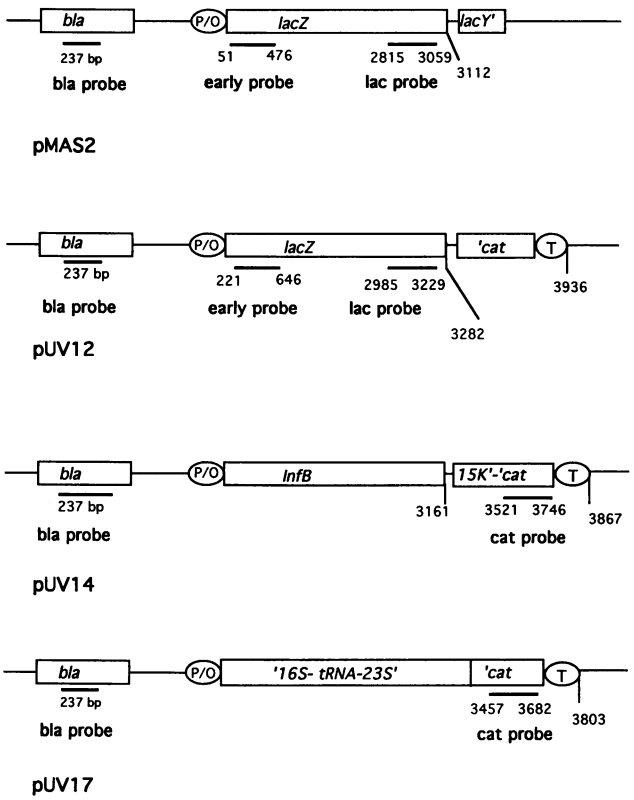

FIG. 1. Schematic presentation of the employed plasmids. Genes are represented by open boxes. P/O, promoter-operator site of either the *lac* promoter on pMAS2 or the $P_{A1/04/03}$ promoter on pUV12, pUV14, and pUV17; T, transcription terminator sequence; ', truncated gene; thick lines, probes complementary to the transcripts at the indicated positions relative to the 5' end. Construction of the plasmids has been described previously (34, 37).

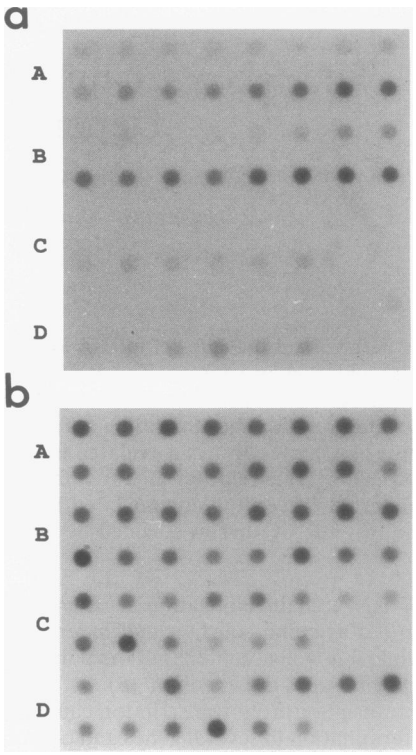

FIG. 2. Autoradiogram of dot blots from induction experiments using MAS90 harboring pMAS2. (a) Hybridization with the *lac* probe; (b) parallel dot blot hybridized with the *bla* probe. Induction was performed during growth on glycerol minimal medium (A and B) or glycerol-Casamino Acids medium (C and D). The dots of this figure are represented in two of the curves in Fig. 3B and two of the curves in Fig. 3C. The major cause for the variation in the intensity of the dots hybridized with the *bla* probe is likely to be traces of phenol left after the ethanol precipitation since equal amounts of A_{260}-absorbing material were applied to each dot and phenol absorbs UV light at 260 nm.

half-life, which differs between the different constructs. Furthermore, since the specific activity of the individual probe, and the hybridization efficiency, varied from time to time, variations in the normalized hybridization levels were seen even between identical experiments. Therefore, in some cases, the results of identical experiments could not be represented in the same panels, and only examples are shown in the figures.)

Riboprobes. The radioactive riboprobes were prepared by in vitro transcription of the corresponding gene segments by use of T7 RNA polymerase and [α-^{32}P]UTP, as described previously (39). The plasmids used for synthesis of the *lacZ* and the *bla* probes are described by Sørensen et al. (34), while the plasmid used for in vitro synthesis of the *cat* riboprobe is described by Vogel and Jensen (37).

RESULTS

Experimental setup. Strain MAS90 overexpresses the *lac* repressor from the F' *lac*^{q1} episome. It was used as genetic background for the different plasmids that all contain a LacI-controlled promoter directing transcription of a gene of considerable length (Fig. 1). The promoter was either the wild-type *lac* promoter (on pMAS2) or the $P_{A1/04/03}$ promoter (on pUV12, pUV14, and pUV17), which is a synthetic derivative of the A1 promoter of the early region of bacteriophage T7 containing two binding sites for the *lac* repressor protein (6a). The employed genes were either *lacZ*, encoding β-galactosidase (on pMAS2 and pUV12); *infB*, encoding the translation initiation factor IF2 (on pUV14); or a major fragment of the *rrnB* operon (on pUV17) encoding an untranslated RNA chain.

To measure the transcription elongation rates, the cultures were induced by addition of IPTG (1 mM) at an optical density at 436 nm of 0.5, and the time elapsing between induction of transcription and the appearance of a specific hybridization signal with the probes complementary to the 3' ends of the transcripts (Fig. 1) was determined by dot blot hybridization, as described in Materials and Methods. The amount of radioactivity hybridizing with the 3' end of the induced RNA chain (i.e., *lacZ* or *cat*) was normalized by dividing by the corresponding amount of radioactivity retained by the constitutive *bla* mRNA and plotted against the sampling time to give an induction curve. The transcription time, which is proportional to the inverse of the RNA chain elongation rate, was defined by the intersection between the horizontal line, seen early after induction, and the steep rising curve that reflects accumulation of full-size RNA chains.

We have previously shown that hybridization complementary to the 5' end of the *lacZ* mRNA encoded by pMAS2, detected by use of the early probe (Fig. 1), appeared very shortly after addition of IPTG and responded only weakly to starvation for isoleucine, which reduces the growth rate by a

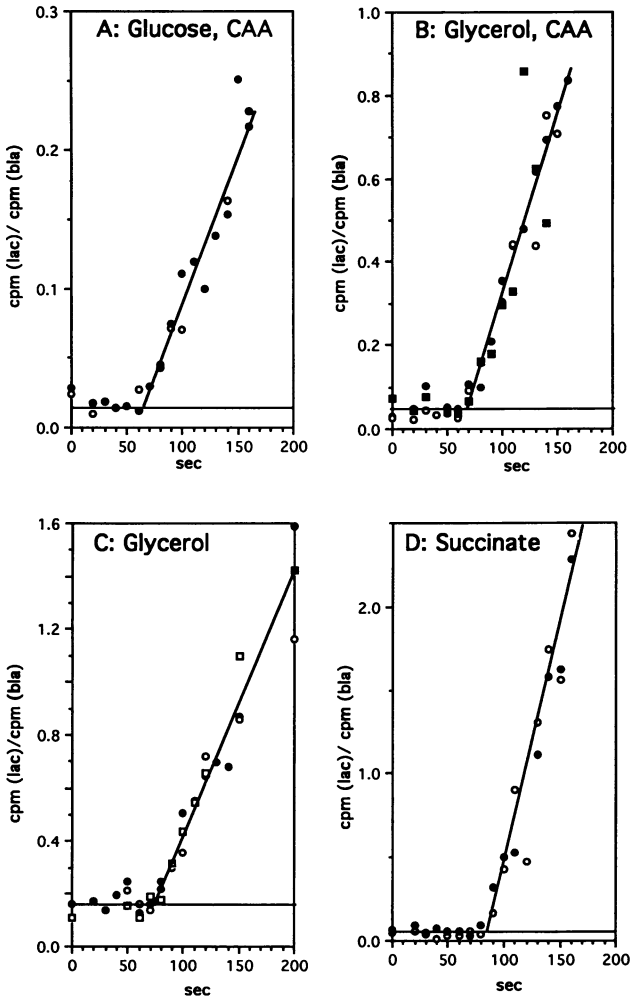

FIG. 3. Induction experiments using MAS90 carrying pMAS2. MAS90 was grown in A+B minimal medium supplied with the carbon sources indicated. At time zero, IPTG was added at 1 mM. RNA was extracted at the indicated times after induction and used for parallel dot blot hybridization with the *lac* probe and the *bla* probe. The amount of radioactivity seen with the *lac* probe was divided by the corresponding radioactivity with the *bla* probe, and the ratio is plotted against sampling time. Data from independent experiments are represented by different symbols. CAA, Casamino Acids.

factor of 3 and the transcript elongation rate by a factor of 2 (39). Similarly, the 5′ ends of *lacZ* transcripts from pUV12 containing the $P_{A1/04/03}$ promoter were quantified by dot blots with the early probe, in exponentially growing and isoleucine-starved cells. Hybridization started to appear as a linear function of time 15 to 20 s after the inducer had been added (data not shown), indicating that the initiation process lasts only a few seconds and that the measured transcription times primarily, if not exclusively, represent RNA chain elongation.

Transcription elongation rates on *lacZ* during growth on different carbon sources. Induction experiments were performed with strain MAS90 transformed with pMAS2, which contains the wild-type *lac* promoter and *lacZ* gene (Fig. 1). Figure 2 shows autoradiographic examples of dot blots from different induction experiments, while Fig. 3 shows the normalized *lacZ* mRNA levels plotted against sampling time to obtain an induction curve. It can be seen that the period

TABLE 1. Induction lags for β-galactosidase and corresponding transcription times for the *lacZ* gene on pMAS2 during steady-state growth

Carbon source	Doubling time (min)	β-Gal induction lag (s)[a] [no. of expts]	*lacZ* transcription time (s)[b] [no. of expts]
Glucose-CAA[c]	35	62 ± 1.2 [3]	60 [2]
Glycerol-CAA	50	67 ± 0.7 [3]	65 [3]
Glycerol	78	75 ± 0.6 [3]	75 [4]
Succinate	160	84 ± 1.0 [5]	85 [2]

[a] The data are means ± standard deviations, determined by the square-root method of Schleif et al. (31). β-Gal, β-galactosidase.
[b] From Fig. 3. Uncertainty, ≈2.5 s.
[c] CAA, 0.2% charcoal-treated Casamino Acids.

between induction and detection of hybridization with the *lac* probe, i.e., the transcription time for *lacZ*, increases from 60 s at a doubling time of 35 min (on glucose-Casamino Acids) to 85 s at a doubling time of 160 min (on succinate minimal medium), corresponding to a >30% change. The intermediate doubling times, i.e., 50 and 78 min, gave rise to transcription times of 70 and 75 s, respectively (Fig. 3). When both glucose and Casamino Acids were present, the measured hybridization with the *lacZ* probe increased only from ca. 25 cpm in the early period after induction to ca. 250 cpm 3 min after addition of IPTG, because of a strong catabolite repression.

Induction lag for β-galactosidase synthesis. Standard induction lags for β-galactosidase synthesis were determined by depicting the square root of the increment in β-galactosidase activity as a function of time after IPTG addition, as described previously (18, 31). The induction lags for β-galactosidase synthesis in the different media are given in Table 1 together with the corresponding transcription times for *lacZ*. It is apparent that the rates of transcription and translation elongation on *lacZ* correlate closely with each other at all growth rates in the employed strain.

Steady-state growth in the presence of α-methylglucoside. In these experiments, the growth rate was varied by adding different amounts of the nonmetabolizable glucose analog α-methylglucoside to the glucose minimal medium, thereby changing the growth rate without changing the carbon source (12, 18).

The transcription time for *lacZ* was determined by using pUV12, which contains *lacZ* fused to the IPTG-inducible $P_{A1/04/03}$ promoter, as shown in Fig. 1. This promoter is not controlled by catabolite repression and gave about 20 times more *lacZ* transcription than the wild-type *lac* promoter. After hybridization with the *lac* probe, the dot blots contained about 50 cpm in the background and up to 15,000 cpm for the latest samples, i.e., 3 to 4 min after induction. The induction curves, shown in Fig. 4, reveal that the transcription time for *lacZ* increased from 75 s on glucose minimal medium (doubling time, 58 min) to 88 s in the presence of a 5-fold excess of α-methylglucoside over glucose (doubling time, 120 min) and 110 s in the presence of a 15-fold excess of α-methylglucoside over glucose (doubling time, 160 min). This corresponds to a ca. 45% increase in the transcription time when the growth rate is reduced 3.3-fold.

Transcription elongation rates on *infB*. To study whether the variation in the transcription elongation rate was specific for the *lacZ* transcript, we used plasmid pUV14, which carries the *infB* gene, encoding translation initiation factor IF2, under control of the LacI-regulated $P_{A1/04/03}$ promoter, as shown in Fig. 1. The 15K gene following *infB* was fused in frame to the

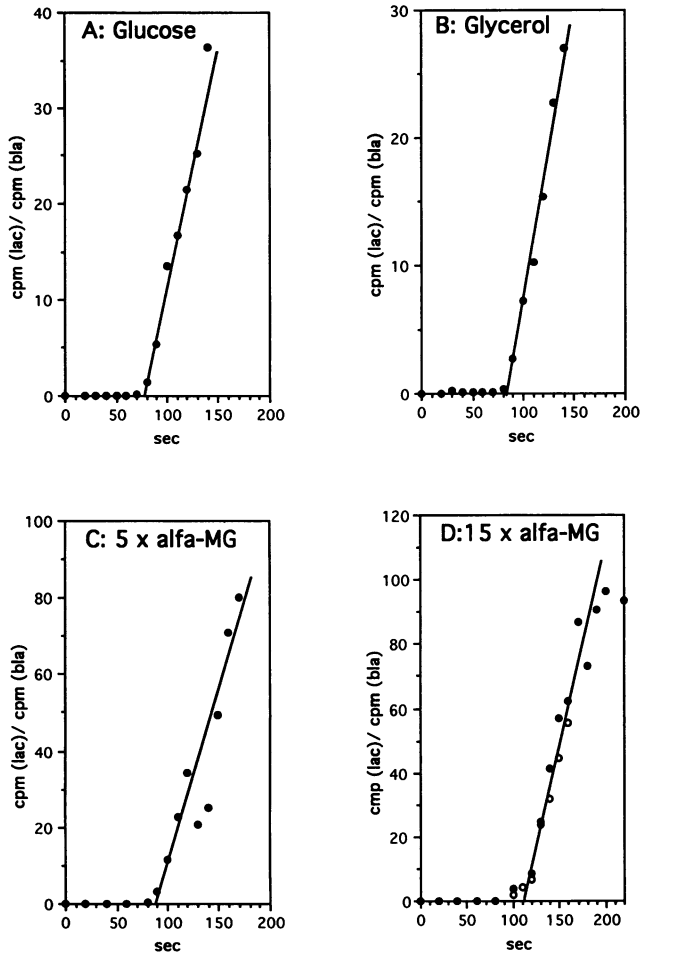

FIG. 4. Induction experiments with MAS90 harboring pUV12 during growth on glucose minimal medium with the indicated α-methylglucoside (alpha-MG)-to-glucose ratios. The experimental procedures were the same as those for Fig. 3. Data from independent experiments are represented by different symbols.

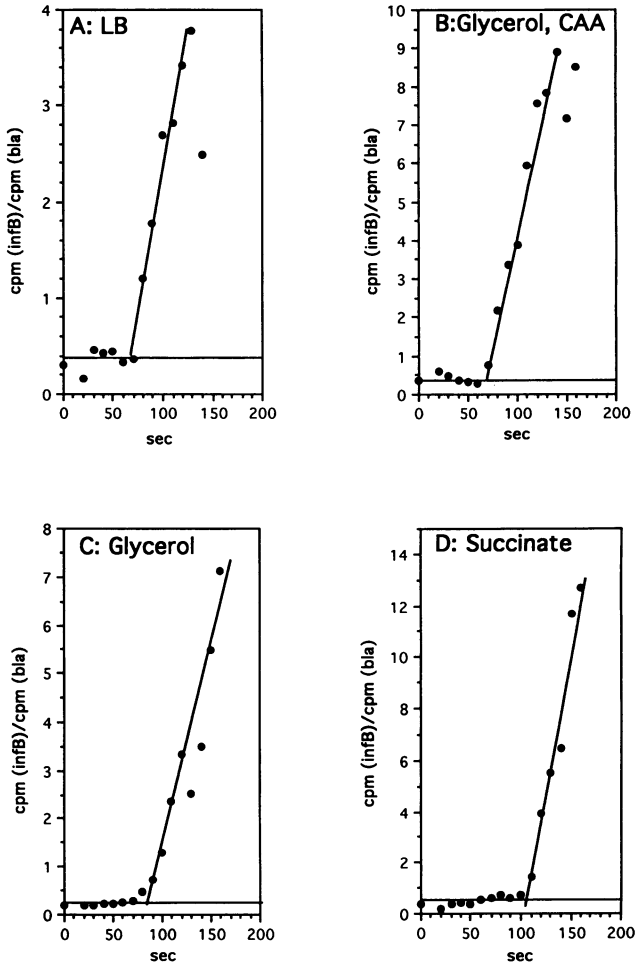

FIG. 5. Induction experiments with MAS90 carrying pUV14 during growth on different carbon sources. The experimental procedures were the same as those for Fig. 3, except that the *cat* probe (Fig. 1) was used to quantify the induced transcript. CAA, Casamino Acids.

cat gene, already present on the vector, and a probe complementary to the truncated *cat* gene (Fig. 1) was used to detect plasmid-specific *infB* transcripts.

Dot blots from induction experiments using pUV14 usually contained about 50 to 100 cpm in the background spots and up to 5,000 cpm in the latest samples. Figure 5 shows the induction curves for the *infB* construct at growth rates ranging from a doubling time of 24 min (in LB broth) to a doubling time of 160 min (in succinate minimal medium). The transcription times were longer with this construct than with pMAS2, since the *cat* probe hybridizes to the *infB* transcript at a mean distance of 3,634 nucleotide residues from the 5′ end of the mRNA while the *lac* probe hybridizes to the *lacZ* transcript at a mean distance of 2,937 nucleotide residues from the 5′ end. It is apparent from Fig. 5 that the transcription time was ca. 70 s in LB broth and 105 s on succinate, corresponding to a 50% variation in the transcription elongation rate. Furthermore, it is interesting that the major effect on the transcription elongation rate is seen at the lower growth rates.

Transcription elongation rates on untranslated RNA. Recently, two widely different estimates (i.e., 42 and 90 nucleotides per second) have been reported for the rate of rRNA chain elongation in LB broth medium (8, 11). In order to measure this parameter by our method, we constructed plasmid pUV17, which contains the central 3,111 bp of the *rrnB* operon inserted after the $P_{A1/04/03}$ promoter and a 20-nucleotide *boxA* sequence in the early part of the transcribed region (37). This minimal *boxA* sequence was previously shown to be sufficient for suppression of Rho-dependent termination in vivo on multicopy plasmids (4) and in vitro (35). Moreover, the *rrnB* DNA on pUV17 was fused to the 3′ part of the *cat* gene in order to obtain a unique sequence for detection of plasmid-specific transcripts (Fig. 1). The probe complementary to the 3′ part of *cat* hybridizes with the transcript at nucleotides 3457 to 3682 from the 5′ end, giving an RNA chain of similar size as the *lacZ* and *infB* transcripts. Northern (RNA) blots, performed as previously described (39), revealed an RNA band accumulating just below the position of 23S RNA upon induction with IPTG (data not shown). The size of this band corresponds to the expected size of a pUV17-specific *rrn* transcript from which the 16S RNA part has been removed by cotranscriptional processing, as for the native *rrn* transcripts (10, 13).

Induction experiments with pUV17 were performed during growth on three different media. The resulting curves are

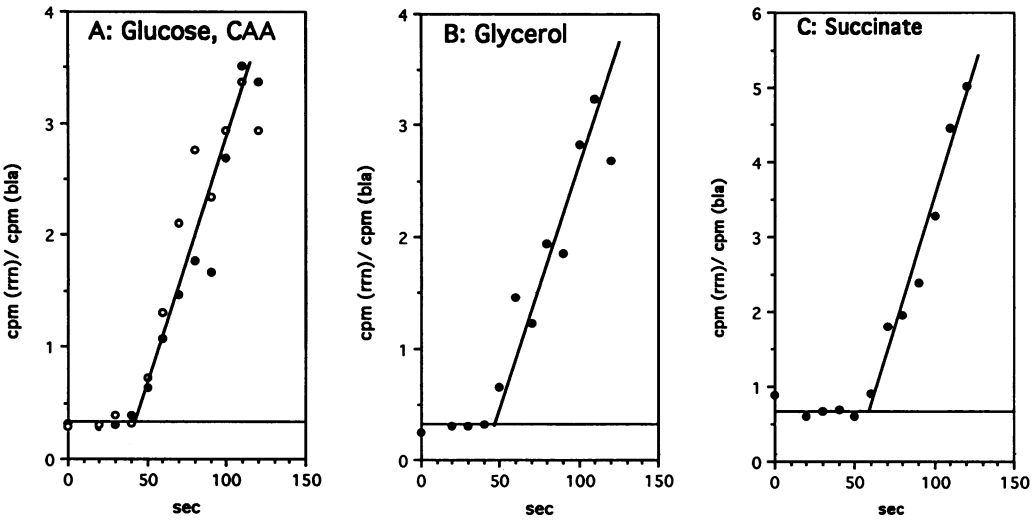

FIG. 6. Induction experiments with MAS90 carrying pUV17 during growth on different carbon sources. The experimental procedures were the same as those for Fig. 3, except that the *cat* probe (Fig. 1) was used to quantify the induced transcript. All the induction experiments were performed twice independently with similar transcription times. CAA, Casamino Acids.

shown in Fig. 6. For unknown reasons (a weak internal promoter?), the uninduced level of hybridization was considerably higher for this construct than those for the other plasmids, i.e., pMAS2, pUV12, and pUV14. The background generally contained 500 to 1,000 cpm, while dots contained about 6,000 cpm ca. 3 min after induction. The transcription time for the *rrnB* gene on pUV17 is much shorter than for the two translated RNA species, *infB* and *lacZ*, being 40 s on glucose-Casamino Acids medium (doubling time, 35 min) and between 50 and 60 s on succinate (doubling time, 160 min).

DISCUSSION

The results in this study indicate strongly that the elongation rates of two different mRNAs and of an untranslated RNA change with the growth rate. The data indicate that the transcription elongation rate increases by 50% when the doubling time is increased sixfold. The small magnitude of this variation may explain why other researchers previously addressing this question concluded that the RNA chain elongation rate was invariant (6, 25, 26), since they were looking for differences proportional to the growth rate differences.

The RNA chain growth rates, measured herein, are compiled in Table 2. It appears that the two mRNAs, i.e., *infB* and *lacZ*, were elongated at similar, but not identical, rates while the untranslated *rrnB-cat* RNA chain was elongated nearly twice as fast. However, the elongation of all three RNA chains varied as a function of growth rate. It is possible that individual genes generally support different transcription rates, as seen for the elongation of individual protein chains in *E. coli* (27), and the large deviation of the transcription elongation rate on the *rrnB-cat* fusion from the other two genes is likely to reflect the unique nature of the nucleotide sequences of *rrn* operons. The high rate of RNA chain elongation on these genes may be due to the fact that the antitermination factors, proposed to associate with the transcription complex at the *boxA* sequence (4, 35), make RNA polymerase resistant to transcriptional pausing, or it may simply be that the *rrn* operons have been selected to be devoid of Rho-dependent terminators and transcriptional pause sites, which often are the same sites (32).

The data for the elongation rate of untranslated RNA agree with some previous estimates reported by Molin (25) and Condon et al. (8). Both these authors estimated the rate of transcription elongation on rRNA operons from the time between rifampin addition to stop new initiation of transcription and cessation of incorporation of radioactive nucleotides in a small RNA species at the end or in the middle of the operon. Condon et al. (8) examined growth only on LB broth and found a transcription elongation rate of 90 nucleotides per s, in agreement with our results (Table 2). Molin (25) studied the RNA chain elongation rate in cultures that took between 75 min and 26 min to double and concluded that the rate of transcription elongation did not depend on the growth rate, although he did observe a 20% difference between the different media (25).

Our results solve the seemingly unnoticed contradiction between, on the one hand, the variable translation elongation rate paired with the dogma of a constant transcription elongation rate and, on the other hand, the well-known polarity effects of decoupling translation from transcription (1) as both parameters change in parallel so that translation remains tightly coupled to transcription at all growth rates (Table 1).

TABLE 2. Rates of transcription elongation

Medium[a]	Doubling time (min)	Transcript elongation (residues/s) on[b]: pMAS2 (2,937)	pUV12 (3,107)	pUV14 (3,634)	pUV17 (3,570)
LB broth	24	—[c]	—	55	—
Glucose-Casamino Acids	35	49	—	—	89
Glycerol-Casamino Acids	50	45	—	53	—
Glycerol	78	39	38	43	79
Succinate	160	35	—	35	66
Glucose	58	—	41	—	—
Glucose–5× αMG[d]	120	—	35	—	—
Glucose–15× αMG	200	—	28	—	—

[a] Described in Materials and Methods.
[b] Numbers of residues from the 5′ end of the transcript to the middle of the hybridization probes shown in Fig. 1 are indicated in parentheses.
[c] —, not determined.
[d] αMG, α-methylglucoside.

We have previously found that the rate of mRNA chain elongation was halved during amino acid starvation of a Rel^+ strain that accumulated vast amounts of ppGpp and that it increased during amino acid starvation of a *relA* mutant, whose ppGpp pool decreased from the basal level to near nothing (37, 39). These observations showed that ppGpp is an inhibitor of mRNA chain elongation in vivo (37) and, as the size of the ppGpp pool increases with decreasing growth rate (3, 5, 9), ppGpp is likely to be responsible for reducing the mRNA elongation rate at the lower growth rates, although other factors, like e.g., the nucleoside triphosphate pools which were shown to decrease with decreasing growth rate (2), also may contribute. Thus, it seems that one very important function of ppGpp in vivo is to maintain a tight coupling of translation to transcription, and it was recently shown that transcription elongation even may limit ribosome movement when high intracellular pools of ppGpp are present (33). Conversely, conditions that reduce mRNA chain elongation or synthesis, like pyrimidine starvation or rifampin treatment, have been shown to result in decreased ppGpp pools (15, 38), indicating that constraints on the mRNA supply make the ribosomes more saturated with substrates. This regulatory interplay between the ppGpp pool and RNA chain elongation seems plausible since growth conditions, or shifts, that lead to shortage of ribosome substrates (e.g., amino acid starvation) cause high ppGpp pools and, thus, inhibit mRNA chain growth and synthesis. In turn, this prevents premature mRNA chain termination, and in addition, it has the consequence that the ribosomes become limited by the mRNA supply and, hence, starve less severely and make fewer translational errors than they would have done without ppGpp accumulation (33).

Jensen and Pedersen (17) have proposed a model for a passive-regulation gene expression under steady-state growth conditions and nutritional shifts, which may contribute to the understanding of the control of ribosome synthesis, which increases with increasing growth rates (30), the regulation of "gearbox promoter" activity which becomes reduced at increasing growth rates (36), and the regulation of other genes whose expression depends on the growth rate (28). According to that model (17), the level of transcription initiation at a single promoter is regulated by avid competition with the many other promoters on the genome for a limited amount of free RNA polymerase, and it was assumed that the concentration of free RNA polymerase increases with the growth rate because of a combination of an increased rate of RNA polymerase synthesis, an increased rate of transcription elongation, and shutdown of biosynthetic gene expression in the richer media (17). The results herein are in agreement with that proposal, since transcription elongation does occur more slowly when the growth rate is reduced. However, the differences in RNA chain elongation are small, suggesting that shutdown of gene expression and the elevated amounts of RNA polymerase per genome equivalent at the high growth rates are more important for the overall growth rate regulation, as originally proposed by Maaløe and coworkers (14, 21, 22, 30).

The relative effect of a 50% variation in the transcription elongation rate on the pool of free RNA polymerase in the cells depends on the actual size of this pool, which is unknown. Although it appears that only 15 to 30% of the total RNA polymerase is engaged in actual RNA chain synthesis, the pool of free RNA polymerase could still be very low, since much of the enzyme may be bound at promoters and since there is only about one (0.5 to 1.5) molecule of the enzyme per promoter in *E. coli*, according to the data of Bremer and Dennis (5) if the genome contains ca. 2,000 promoters. On the other hand, McClure (23) has estimated that the functional concentration of free RNA polymerases in the cell is ca. 30 nM, corresponding to about 20 free RNA polymerases per genome. This estimate was made by correlating the predicted initiation frequencies, calculated from the in vitro properties of a series of promoters, with their relative initiation frequencies in vivo, measured by use of *lacZ* fusions (23). There seems to be a very large discrepancy between this estimate of McClure (23) and the thousands of nontranscribing RNA polymerases that are present in the cell according to Bremer and Dennis (5), and the question of why so many nontranscribing RNA polymerases behave as if only 20 of them were available for initiation of new RNA chain synthesis inside the cell remains open. That question seems to be of key importance for understanding the regulation of ribosomal operons and other growth rate-regulated genes.

ACKNOWLEDGMENTS

We thank Michael Sørensen (University of Copenhagen) for strain MAS90.

This work was supported financially by a grant from the Danish Center of Microbiology.

REFERENCES

1. **Adhya, S., and M. Gottesman.** 1978. Control of transcription termination. Annu. Rev. Biochem. **47**:967–996.
2. **Bagnara, A. S., and L. R. Finch.** 1973. Relationships between intracellular contents of nucleotides and 5-phosphoribosyl-1-pyrophosphate in *Escherichia coli*. Eur. J. Biochem. **36**:422–427.
3. **Baracchini, E., and H. Bremer.** 1988. Stringent and growth control of rRNA synthesis in *Escherichia coli* are both mediated by ppGpp. J. Biol. Chem. **263**:2597–2602.
4. **Berg, K. L., C. Squires, and C. L. Squires.** 1989. Ribosomal RNA operon anti-termination. Function of leader and spacer region BoxB-BoxA sequences and their conservation in diverse microorganisms. J. Mol. Biol. **209**:345–358.
5. **Bremer, H., and P. P. Dennis.** 1987. Modulation of chemical composition and other parameters of the cell by growth rate, p. 1527–1542. *In* F. C. Neidhardt, J. C. Ingraham, K. B. Low, B. Magasanik, M. Schaechter, and H. E. Umbarger (ed.), *Escherichia coli* and *Salmonella typhimurium*: cellular and molecular biology. American Society for Microbiology, Washington, D.C.
6. **Bremer, H., and D. Yuan.** 1968. RNA chain growth-rate in *Escherichia coli*. J. Mol. Biol. **38**:163–180.

6a. **Bujard, H.** Personal communication.

7. **Clark, D. J., and O. Maaløe.** 1967. DNA replication and the division cycle of *Escherichia coli*. J. Mol. Biol. **23**:99–112.
8. **Condon, C., S. French, C. Squires, and C. L. Squires.** 1993. Depletion of functional ribosomal RNA operons in *Escherichia coli* causes increased expression of the remaining intact operons. EMBO J. **12**:4305–4315.
9. **Fiil, N. P., K. V. Meyenburg, and J. D. Friesen.** 1972. Accumulation and turnover of guanosine tetraphosphate in *Escherichia coli*. J. Mol. Biol. **71**:769–783.
10. **French, S. L., and O. L. J. Miller.** 1989. Transcription mapping of the *Escherichia coli* chromosome by electron microscopy. J. Bacteriol. **171**:4207–4216.
11. **Gotta, S., O. L. Miller, Jr., and S. L. French.** 1991. rRNA transcription rate in *Escherichia coli*. J. Bacteriol. **173**:6647–6649.
12. **Hansen, M. T., M. L. Pato, S. Molin, N. P. Fiil, and K. von Meyenburg.** 1975. Simple downshift and resulting lack of correlation between ppGpp pool size and ribonucleic acid accumulation. J. Bacteriol. **122**:585–591.
13. **Hofmann, S., and O. L. Miller, Jr.** 1977. Visualization of ribosomal ribonucleic acid synthesis in a ribonuclease III-deficient strain of *Escherichia coli*. J. Bacteriol. **132**:718–722.
14. **Ingraham, J. L., O. Maaløe, and F. C. Neidhardt.** 1983. Growth of the bacterial cell. Sinauer Associates, Inc., Sunderland, Mass.
15. **Jensen, K. F.** Unpublished observations.
16. **Jensen, K. F., F. Bonekamp, and P. Poulsen.** 1986. Attenuation at nucleotide biosynthetic genes and amino acid biosynthetic operons

of *Escherichia coli*. Trends Biochem. Sci. **11**:362–365.
17. **Jensen, K. F., and S. Pedersen.** 1990. Metabolic growth rate control in *Escherichia coli* may be a consequence of subsaturation of the macromolecular biosynthetic apparatus with substrates and catalytic components. Microbiol. Rev. **54**:89–100.
18. **Johnsen, K., S. Molin, O. Karlström, and O. Maaløe.** 1977. Control of protein synthesis in *Escherichia coli*: analysis of an energy source shift-down. J. Bacteriol. **131**:18–29.
19. **Landick, R., J. Carey, and C. C. Yanofsky.** 1985. Translation activates the paused transcription complex and restores transcription of the *trp* operon leader region. Proc. Natl. Acad. Sci. USA **82**:4663–4667.
20. **Landick, R., and C. Yanofsky.** 1987. Transcription attenuation, p. 1276–1301. *In* F. C. Neidthardt, J. C. Ingraham, K. B. Low, B. Magasanik, M. Schaechter, and H. E. Umbarger (ed.), *Escherichia coli* and *Salmonella typhimurium*: cellular and molecular biology. American Society for Microbiology, Washington, D.C.
21. **Maaløe, O.** 1979. Regulation of the protein synthesizing machinery—ribosomes, tRNA, factors, and so on, p. 487–542. *In* R. F. Goldberger (ed.), Biological regulation and development. Plenum Publishing Corp., New York.
22. **Maaløe, O., and N. O. Kjeldgaard.** 1966. Control of macromolecular synthesis: a study of DNA, RNA, and protein synthesis in bacteria. Benjamin, New York.
23. **McClure, W. R.** 1983. A biochemical analysis of the effect of RNA polymerase concentration on the *in vivo* control of RNA chain initiation frequency, p. 207–217. *In* D. L. F. Lennon, F. W. Stratman, and R. N. Zahlten (ed.), Biochemistry of metabolic processes. Elsevier Science Publishing Co., Inc., New York.
24. **Miller, J. H.** 1972. Experiments in molecular genetics. Cold Spring Harbor Laboratory, Cold Spring Harbor, N.Y.
25. **Molin, S.** 1976. Ribosomal RNA chain elongation in *Escherichia coli*, p. 333–337. *In* N. O. Kjeldgaard and O. Maaløe (ed.), Alfred Benzon symposium IX. Academic Press, Inc., New York.
26. **Molin, S., K. von Meyenburg, O. Maaløe, M. T. Hansen, and M. L. Pato.** 1977. Control of ribosome synthesis in *Escherichia coli*: analysis of an energy source shift-down. J. Bacteriol. **131**:7–17.
27. **Pedersen, S.** 1984. *Escherichia coli* ribosomes translate in vivo with variable rate. EMBO J. **3**:2895–2898.
28. **Pedersen, S., P. L. Bloch, S. Reeh, and F. C. Neidhardt.** 1978. Patterns of protein synthesis in *E. coli*: a catalog of the amount of 140 individual proteins at different growth rates. Cell **14**:179–190.
29. **Roland, K. L., C. Liu, and C. L. Turnbough.** 1988. Role of the ribosome in suppressing transcriptional termination at the *pyrBI* attenuator of *Escherichia coli* K-12. Proc. Natl. Acad. Sci. USA **85**:7149–7153.
30. **Schaechter, M., O. Maaløe, and N. O. Kjeldgaard.** 1958. Dependency on medium and temperature of cell size and chemical composition during balanced growth of *Salmonella typhimurium*. J. Gen. Microbiol. **19**:592–606.
31. **Schleif, R., W. Hess, S. Finkelstein, and D. Ellis.** 1973. Induction kinetics of the L-arabinose operon of *Escherichia coli*. J. Bacteriol. **115**:9–14.
32. **Sigmund, C. D., and E. A. Morgan.** 1988. NusA protein affects transcriptional pausing and termination in vitro by binding to different sites on the transcription complex. Biochemistry **27**:5622–5627.
33. **Sørensen, M. A., K. F. Jensen, and S. Pedersen.** 1994. High concentrations of ppGpp decrease the RNA chain growth rate: implications for protein synthesis and translational fidelity during amino acid starvation in *Escherichia coli*. J. Mol. Biol. **236**:441–454.
34. **Sørensen, M. A., C. G. Kurland, and S. Pedersen.** 1989. Codon usage determines the translation rate in *Escherichia coli*. J. Mol. Biol. **207**:365–377.
35. **Squires, C. L., J. Greenblatt, J. Li, C. Condon, and C. L. Squires.** 1993. Ribosomal RNA antitermination *in vitro*: requirement for Nus factors and one or more unidentified cellular components. Proc. Natl. Acad. Sci. USA **90**:970–974.
36. **Vincente, M., S. R. Kushner, T. Garrido, and M. Aldea.** 1991. The role of the "gearbox" in the transcription of essential genes. Mol. Microbiol. **5**:2085–2091.
37. **Vogel, U., and K. F. Jensen.** Effects of guanosine 3′,5′-bisdiphosphate on the rate of transcription elongation in isoleucine starved *Escherichia coli*. Submitted for publication.
38. **Vogel, U., S. Pedersen, and K. F. Jensen.** 1991. An unusual correlation between the ppGpp pool size and the rate of ribosome synthesis during partial pyrimidine starvation of *Escherichia coli*. J. Bacteriol. **173**:1168–1174.
39. **Vogel, U., M. Sørensen, S. Pedersen, K. F. Jensen, and M. Kilstrup.** 1992. Decreasing transcription elongation rate in *Escherichia coli* exposed to amino acid starvation. Mol. Microbiol. **6**:2191–2200.